IEEE Access
Multidisciplinary | Rapid Review | Open Access Journal

Received 30 March 2024, accepted 3 May 2024, date of publication 17 May 2024, date of current version 24 May 2024.

Digital Object Identifier 10.1109/ACCESS.2024.3402379

RESEARCH ARTICLE

Self-Adjusting Prescribed Performance H∞ Trajectory Tracking Control for Underactuated Autonomous Underwater Vehicles

JIAOYANG ZHUO, HAITAO LIU, (Member, IEEE), XUEHONG TIAN, AND QINGQUN MAI

School of Mechanical Engineering, Guangdong Ocean University, Zhanjiang 524088, China
Shenzhen Institute, Guangdong Ocean University, Shenzhen 518120, China
Guangdong Provincial Key Laboratory of Intelligent Equipment for South China Sea Marine Ranching, Guangdong Engineering Technology Research Center of Ocean Equipment and Manufacturing, Zhanjiang 524088, China

Corresponding authors: Haitao Liu (gdliuht@126.com) and Qingqun Mai (qingqmai@163.com)

This work was supported in part by Guangdong Basic and Applied Basic Research Foundation under Grant 2024A1515011345, in part by Shenzhen Science and Technology Program under Grant JCYJ20220530162014033, in part by the Key Project of the Department of Education of Guangdong Province under Grant 2023ZDZX1005 and Grant 2021ZDZX1041, in part by the National Natural Science Foundation of China under Grant 62171143, and in part by the Science and Technology Planning Project of Zhanjiang City under Grant 2021A05023 and Grant 2021E05012.

ABSTRACT A predefined-time H_∞ trajectory tracking control scheme based on self-adjusting prescribed performance functions and dynamic relative threshold event-triggered mechanism is proposed for a five-degree-of-freedom underactuated autonomous underwater vehicle (AUV) with unknown external disturbances and actuators saturated. First, a new self-adjusting prescribed performance function is designed to ensure that the tracking errors do not exceed the prescribed bounds and to solve the singularity problem of general prescribed performance control (PPC) due to actuator saturation. Second, a predefined-time H_∞ controller combined with a predefined-time dynamic surface control (DSC) method is proposed to guarantee that system signals converge to the neighborhood of zero in a predefined time without adjusting the control parameters and to improve system robustness to uncertain disturbances. Third, an improved dynamic relative threshold event-triggered method is designed to save the communication resources of an underactuated AUV system. Then, the Lyapunov stability proof indicates that all signals in the closed-loop system are predefined-time bounded, and the trajectory tracking errors can converge to the neighborhood of zero within the set desired time. Finally, the simulations not only demonstrate the performance of the proposed controller-controlled system but also verify the effectiveness of the proposed scheme.

INDEX TERMS Underactuated autonomous underwater vehicle, predefined-time control, H_∞ control, trajectory tracking, prescribed performance control.

I. INTRODUCTION

The ocean occupies more than 70% of the Earth's surface and is rich in mineral and underwater biological resources. Autonomous underwater robots are important tools for realizing undersea work, such as ocean exploration, target detection, and exploration missions. Underactuated AUVs reduce the number and complexity of mechanical components in their mechanical structure, which reduces energy consumption and energy demand for system operation, improves energy utilization efficiency, and reduces the number of failure points, which makes underactuated AUVs more reliable and durable in extreme environments [1], [2]. Therefore, the study of underactuated AUVs could provide a more sustainable solution for marine scientific research, resource exploration and environmental monitoring, among other areas.

The associate editor coordinating the review of this manuscript and approving it for publication was Zhiguang Feng.

Trajectory tracking control research is the basis for underactuated AUVs to accomplish various underwater operations, and it is a major research topic in the field of motion control [1], [2]. Therefore, research on trajectory tracking control of underactuated AUV systems is very important for practical applications. However, underactuated AUV models are highly nonlinear, strongly coupled and suffer from the problem of current interference in the marine environment, and many control algorithms are unable to achieve the desired control effect on underactuated AUV systems because of the lack of system actuators [3], [4]. It is of great research value and significance to design controllers to ensure smooth and reliable trajectory tracking of underactuated AUV systems in complex marine environments.

Several control schemes have been proposed to solve the problem of underactuated AUV trajectory tracking control in the presence of external uncertainty disturbances and actuator saturation. Elhaki and Shojaei proposed a backstepping controller with a robust multilayer neural network to estimate disturbances [5]. Sun et al. designed a fixed-time sliding mode controller and a fixed-time sliding extended state observer to compensate for external disturbances [6]. Yan et al. used an observer controller and a radial basis function neural network to compensate for external disturbances [7]. An adaptive prescribed performance tracking controller was designed in [8] and [9]. The controllers mentioned above are basically finite-time or fixed-time stable, and in the processing of external disturbances, a neural network or observer is used for compensation to enhance the robustness of the whole system. However, the convergence time of finite-time control algorithms is affected by the initial state of the system, and the estimated convergence time of a fixed-time control algorithm is usually inaccurate and conservative. Moreover, the convergence time is not explicitly related to the adjustable parameters of the controller. Therefore, predefined-time control methods were proposed in [10], [11], [12], and [13] to make a system converge to the steady state in a predefined time without relying on the initial value of the system. The convergence time does not need to be calculated in a complicated way, and the convergence time can be adjusted by controlling the parameters. The addition of observers and neural networks increases the complexity of the control system, and the computational burden of the system increases significantly, making it difficult to use in scenarios where real-time performance is needed. Therefore, a finite-time robust H_∞ control method was proposed by Liu et al. to suppress external disturbances [14]. Wang et al. further proposed a fixed-time H_∞ controller to decrease the interference of observation errors [15]. These references [16], [17], [18], and [19] also used the robust H_∞ control method to strengthen the robustness of the system. The H_∞ control method can strengthen the robustness of a controller without adding other compensation mechanisms to suppress the disturbance of external uncertainty perturbations, and the control output has a predefined upper-bounded L2 gain. However, in the field of underactuated AUV trajectory tracking control, the H_∞ control method is rarely utilized.

PPC is performed by defining a performance function and introducing error transformations to maintain the tracking error within the boundaries determined by the performance function. PPC is widely used in trajectory tracking control research due to its excellent error bounding capability. References [5], [20], and [21] used the PPC method to constrain errors and achieve the desired tracking effect. Both [22] and [23] designed funnel PPC methods to constrain tracking errors. Funnel-type prescribed performance functions have the advantages of simple calculations and good results. Li et al. proposed an appointed-time performance function to constrain tracking errors [24]. The previous PPC bounds are simple time-varying functions, and in the case of abrupt error changes caused by actuator saturation, the bounds cannot be adjusted according to the error, so there may be singularity problems. Therefore, a performance function was designed by Bu et al. by adaptively regulating the constraint [25]. A PPC method with an adjustable boundary was also designed in [26], and both of them used a ln-type performance function, but the ln-type performance function is complicated to calculate.

The event-triggered method can effectively save the communication resources of a system, so it is used extensively in the control field. The system state and controller of a traditional control system are acquired in a fixed sampling period, but when the system is stable, the system state changes remain flat, and if the same sampling method is still used, many communication resources will be wasted. Therefore, the event-triggered method was introduced [27]. The sampling and transmission of a system state occurs when the trigger condition is established. A fault evaluation method with an integrating event-triggered scheme was applied to an AUV control system to improve the safety and reliability of the system [28]. In [29], the X-Z coordinates and pitch angle were delivered in an event-triggered manner, and an event-triggered adaptive neuro-observer was established to effectively save communication resources. Bian et al. proposed a self-triggering mechanism to reduce the computational and communication load, and the trigger interval was the maximum time interval that satisfied the termination constraint [30]. A distribution event-triggered formation control method with asynchronous periodic sampling control approaches was designed to achieve discrete and lead-free multi-AUV distributed formation control to save communication resources in [31].

Inspired by the aforementioned papers and based on self-adjusting prescribed performance functions and a dynamic relative threshold event-triggered mechanism, a predefined-time H_∞ trajectory tracking control scheme is proposed for a five-degree-of-freedom underactuated AUV with unknown external disturbances and actuator saturation. The main characteristics and contributions of this essay can be summarized as follows:

(1) An innovative self-adjusting prescribed performance control method is proposed to overcome the singularity problem of the conventional PPC method due to actuator saturation. Compared with reference [26], the performance function is improved, and a judgment mechanism is added as a way to overcome the boundary divergence problem due to excessive actuator saturation in underactuated systems. Different from the functions in references [25] and [26], a simpler and more widely applicable error conversion function is employed to implement peer-to-peer conversion of performance-constrained spaces to unconstrained space.

(2) A robust predefined-time H_∞ control strategy is proposed to improve the robustness of the system to reduce the negative effects of uncertain disturbances, including external environment disturbances, actuator saturation and model uncertainties. Different from the fixed-time method [15], the predefined-time controller can converge in a predefined time without complex calculations. Compared with the predefined-time controller in [32], the predefined-time controller proposed in this paper has better control accuracy. Moreover, a predefined-time dynamic surface control method is proposed to solve the computational explosion problem. Under the action of the proposed predefined-time H_∞ controller and the predefined-time dynamic surface control method, the whole closed-loop system is predefined-time stable and has strong anti-jamming ability and high tracking accuracy.

(3) An improved dynamic relative threshold event-triggered mechanism is proposed to further reduce the communication pressure by a dynamic function that adjusts the execution interval. Compared with the mechanism in references [32] and [33], the proposed event-triggered mechanism is a more efficient compensation mechanism and can better convert communication resources. Moreover, the proposed event-triggered mechanism guarantees that the proposed event-triggered controller still has the same performance as the time-triggered mechanism.

The entire paper is divided into six chapters. The first chapter is the introduction section. The second chapter describes the theoretical aspects and significant fundamental concepts. The main results are provided in Section III, and the self-adjusting prescribed performance control method, predefined-time dynamic surface control method, predefined-time H_∞ controller design and dynamic relative threshold event-triggered mechanism are detailed. Section IV provides the stability proof, where the predefined-time stability of all signals in the closed-loop system is proven first, and then the predefined-time stability of all signals in the closed-loop system after an event trigger is verified; finally, it is proven that no zeno behavior exists. The simulation results are provided in Section V to demonstrate the feasibility and effectiveness of the proposed method. Finally, a brief summary of the paper is given in the conclusion in Section VI.

II. PRELIMINARIES

A. UNDERACTUATED AUV KINEMATICS AND DYNAMICS MODEL

Focusing on a 5-DOF underactuated AUV model with external environmental interferences and actuator saturation, the kinematic and dynamic models of the underactuated AUV model can be presented as follows:

$$\begin{aligned}&\dot{\eta} = J(\eta)\bar{v}\\ &M\dot{\bar{v}} + C(\bar{v})\bar{v} + D(\bar{v})\bar{v} + g(\eta) = \tau + \omega\end{aligned} \tag{1}$$

where $\eta = [x, y, z, \Theta, \varphi]^T$ is the position and orientation of the vehicle, $\bar{v} = [u, \upsilon, w, q, r]^T$ is the vector of the velocities, $M \in \Re^{5\times5}$ denotes the inertia matrix, $g(\eta) \in \Re^{5\times5}$ is the vector of the buoyancy and gravity forces, $C(\bar{v}) \in \Re^{5\times5}$ contains Coriolis terms, $D(\bar{v}) \in \Re^{5\times5}$ is the damping force and torque matrix that is strictly positive [6], [34], [35], [36], [37], $\omega \in \Re^{5\times1}$ represents the unknown external interference and $\tau \in \Re^{5\times1}$ represents the vector of actuator inputs. According to reference [38], the following equations hold:

$$J(\eta) = \begin{bmatrix} \cos\varphi\cos\Theta, & -\sin\varphi, & \sin\Theta\cos\varphi, & 0, & 0\\ \sin\varphi\cos\Theta, & \cos\varphi, & \sin\Theta\sin\varphi, & 0, & 0\\ -\sin\Theta, & 0, & \cos\Theta, & 0, & 0\\ 0, & 0, & 0, & 1, & 0\\ 0, & 0, & 0, & 0, & \frac{1}{\cos\Theta} \end{bmatrix} \tag{2}$$

$$M = \begin{bmatrix} m_{11}, & 0, & 0, & 0, & 0\\ 0, & m_{22}, & 0, & 0, & 0\\ 0, & 0, & m_{33}, & 0, & 0\\ 0, & 0, & 0, & m_{55}, & 0\\ 0, & 0, & 0, & 0, & m_{66} \end{bmatrix},$$

$$C(v) = \begin{bmatrix} 0, & 0, & 0, & m_{33}w, & -m_{22}\upsilon\\ m_{11}r, & 0, & 0, & 0, & 0\\ 0, & -m_{11}u, & 0, & 0, & 0\\ (m_{33}-m_{11})w, & 0, & 0, & 0, & 0\\ (m_{11}-m_{22})\upsilon, & 0, & 0, & 0, & 0 \end{bmatrix},$$

$$D(v) = \begin{bmatrix} d_{11}, & 0, & 0, & 0, & 0\\ 0, & d_{22}, & 0, & 0, & 0\\ 0, & 0, & d_{33}, & 0, & 0\\ 0, & 0, & 0, & d_{55}, & 0\\ 0, & 0, & 0, & 0, & d_{66} \end{bmatrix},$$

$$g(\eta) = \begin{bmatrix} 0\\ 0\\ 0\\ \rho\bar{g}\Delta\overline{GM_L}\sin\Theta\\ 0 \end{bmatrix}, \tau = \begin{bmatrix} \tau_u\\ 0\\ 0\\ \tau_q\\ \tau_r \end{bmatrix} \tag{3}$$

Substituting Eqs. (2) and (3) into Eq. (1), a detailed expansion of (1) can be expressed as:

$$\begin{cases} \dot{x} = u\cos\varphi\cos\Theta + w\sin\Theta\cos\varphi - \upsilon\sin\varphi\\ \dot{y} = w\sin\Theta\sin\varphi + u\sin\varphi\cos\Theta + \upsilon\cos\varphi\\ \dot{z} = -u\sin\Theta + w\cos\Theta\\ \dot{\Theta} = q\\ \dot{\varphi} = r/\cos\Theta \end{cases} \tag{4}$$

$$\begin{cases} m_{11}\dot{u} - m_{22}\upsilon r + m_{33}wq + d_{11}u = \tau_u + \omega_u \\ m_{11}ur + m_{22}\dot{\upsilon} + d_{22}\upsilon = \omega_\upsilon \\ m_{33}\dot{w} + d_{33}w - m_{11}u\mathrm{q} = \omega_w \\ m_{55}\dot{q} + \rho\bar{g}\Delta\overline{GM_L}\sin\Theta + d_{55}q - (m_{33} - m_{11})uw \\ = \tau_q + \omega_q \\ m_{66}\dot{r} + d_{66}r - (m_{11} - m_{22})u\upsilon = \tau_r + \omega_r \end{cases} \tag{5}$$

where the details of each parameter are the same as those in [22] and [39].

Remark 1: The AUV is equipped with a separate external actuator to drive at low speeds. It is reasonable to ignore the rolling dynamics of the six-degree-of-freedom AUV, so the above five-degree-of-freedom AUV is used to simplify the model. A more detailed explanation can be found in the literature [40]. This 5-degree-of-freedom AUV model has been discussed many times in 3D space motion control, including for trajectory tracking [41], [42], cooperative control [43], [44], and path following [45].

The saturated force or torque input $\tau_{si}(i = u, q, r)$ is defined as follows:

$$\tau_{si} = \begin{cases} \tau_{i\max}, \tau_i > \tau_{i\max} \\ \tau_i, \tau_{i\max} \le \tau_i \le \tau_{i\min} \\ \tau_{i\min}, \tau_i < \tau_{i\min} \end{cases} \tag{6}$$

where τ_{si} is the saturated force or torque, $\tau_{i\min}$ is the minimum value and $\tau_{i\max}$ is the maximum value of the control force or torque. Then,

There is a direct error $\tau_{ie} = \tau_{si} - \tau_{ai}, (i = u, q, r)$ between the saturated force or torque τ_{si} and the actual required force or torque τ_i, and substituting $\tau_{si} = \tau_{ai} + \tau_{ie}$ into Model (3) yields:

$$\begin{cases} m_{11}\dot{u} - m_{22}\upsilon r + m_{33}wq + d_{11}u = \tau_{au} + \tau_{ue} + \omega_u \\ m_{11}ur + m_{22}\dot{\upsilon} + d_{22}\upsilon = \omega_\upsilon \\ m_{33}\dot{w} + d_{33}w - m_{11}u\mathrm{q} = \omega_w \\ m_{55}\dot{q} + G + d_{55}q - (m_{33} - m_{11})uw = \tau_{aq} + \tau_{qe} + \omega_q \\ m_{66}\dot{r} + d_{66}r - (m_{11} - m_{22})u\upsilon = \tau_{ar} + \tau_{re} + \omega_r \end{cases} \tag{7}$$

The uncertainty disturbance function is defined as $f_i(i = u, \upsilon, w, q, r)$ and includes the unknown time-varying external environment interference, model uncertainties and actuator saturation.

$$\begin{cases} f_u = \omega_u - d_{11}\Delta_{d,1}u + m_{22}\Delta_{m,2}\upsilon r - m_{11}\Delta_{m,1}\dot{u} \\ -m_{33}\Delta_{m,3}wq + \tau_{ue} \\ f_\upsilon = \omega_\upsilon - d_{22}\Delta_{d,2}\upsilon - m_{11}\Delta_{m,1}ur - m_{22}\Delta_{m,2}\dot{\upsilon} \\ f_w = \omega_w - d_{33}\Delta_{d,3}w - m_{11}\Delta_{m,1}u\mathrm{q} - m_{33}\Delta_{m,3}\dot{\mathrm{w}} \\ f_q = \omega_q - d_{55}\Delta_{d,5}q - \Delta_g G - m_{55}\Delta_{m,5}\dot{q} \\ -(m_{11}\Delta_{m,1} - m_{33}\Delta_{m,3})uw + \tau_{qe} \\ f_r = \omega_r - d_{66}\Delta_{d,6}r - (\Delta_{m,2}m_{22} - \Delta_{m,1}m_{11})u\upsilon \\ -m_{66}\Delta_{m,6}\dot{r} + \tau_{re} \end{cases} \tag{8}$$

where $h_i \in \Re^{5\times1}, (i = u, \upsilon, w, q, r)$ represents the unknown time-varying external environment disturbance and $\Delta_{d,j}$, $\Delta_{m,j}(j = 1, 2, 3, 5, 6)$, Δ_g represents the model parameter uncertainties.

Thus, the underactuated AUV model in Eq. (5) after considering model uncertainty and actuator saturation is converted into the following form:

$$\begin{cases} m_{11}\dot{u} - m_{22}\upsilon r + m_{33}wq + d_{11}u = \tau_{au} + f_u \\ m_{11}ur + m_{22}\dot{\upsilon} + d_{22}\upsilon = f_\upsilon \\ m_{33}\dot{w} + d_{33}w - m_{11}u\mathrm{q} = f_w \\ m_{55}\dot{q} + G + d_{55}q - (m_{33} - m_{11})uw = \tau_{aq} + f_q \\ m_{66}\dot{r} + d_{66}r - (m_{11} - m_{22})u\upsilon = \tau_{ar} + f_r \end{cases} \tag{9}$$

B. LINE OF SIGHT METHOD DESCRIPTION

The position tracking error in the body coordinate frame is defined as follows:

$$\begin{cases} x_e = -(z - z_h)\sin\Theta + (y - y_h)\cos\Theta\sin\varphi \\ +(x - x_h)\cos\varphi\cos\Theta \\ y_e = (y - y_h)\cos\varphi - (x - x_h)\sin\varphi \\ z_e = (z - z_h)\cos\Theta + (y - y_h)\sin\varphi\sin\Theta \\ +(x - x_h)\cos\varphi\sin\Theta \end{cases} \tag{10}$$

where (x_h, y_h, z_h) is the desired 3D trajectory of the AUV model in this paper. The derivative of Equation (10) yields the following equation:

$$\begin{cases} \dot{x}_e = \mathrm{u} - qz_e + \mathrm{r}y_e + N_x \\ \dot{y}_e = \upsilon - r(x_e + z_e\tan\Theta) + N_y \\ \dot{z}_e = ry_e\tan\Theta + w + qx_e + N_z \end{cases} \tag{11}$$

$$\begin{cases} N_x = -\dot{x}_h\cos\varphi\cos\Theta - \dot{y}_h\sin\varphi\cos\Theta + \dot{z}_h\sin\Theta \\ N_y = \dot{x}_h\sin\varphi - \dot{y}_h\cos\varphi \\ N_z = -\dot{x}_h\cos\varphi\sin\Theta - \dot{y}_h\sin\varphi\sin\Theta - \dot{z}_h\cos\Theta \end{cases} \tag{12}$$

Then, it is assumed that a range sensor is equipped to measure the line-of-sight (LOS) distance ρ_e between the center of mass of the underactuated AUV system and a bearing sensor for measuring the pitch angle θ_e and yaw angle φ_e relative to the target. The LOS distance ρ_e, pitch angle θ_e and yaw angle φ_e are related to the error x_e, y_e, z_e in the fixed-frame body, and they are expressed as:

$$\begin{cases} \rho_e = \sqrt{x_e^2 + y_e^2 + z_e^2} \\ \theta_e = \arctan 2(z_e, \sqrt{x_e^2 + y_e^2}) \\ \varphi_e = \arctan 2(y_e, x_e) \end{cases} \tag{13}$$

The corresponding AUV frame and coordinate diagram are given in Fig. 1. The derivative of Eq. (13) is found and combined with Eqs. (4), (9) and (11), which yields:

$$\begin{cases} \dot{\rho}_e = uL_u + \Phi_u \\ \dot{\theta}_e = qL_q + \Phi_q \\ \dot{\varphi}_e = rL_r + \Phi_r \end{cases} \tag{14}$$

where

$$\begin{cases} L_u = \cos\theta_e \cos\varphi_e \\ L_q = \cos\varphi_e \\ L_r = -(1 + \cos\varphi_e \tan\theta_e \tan\Theta) \end{cases} \tag{15}$$

$$\begin{cases} \Phi_u = \upsilon\cos\theta_e \sin\varphi_e + w\sin\theta_e \\ +N_x \cos\theta_e \cos\varphi_e \\ +N_y \cos\theta_e \sin\varphi_e + N_z \sin\theta_e \\ \Phi_q = \dfrac{\cos\theta_e(w + N_z)}{\rho_e} + r\tan\Theta\sin\varphi_e \\ -\dfrac{u\cos\varphi_e \sin\theta_e}{\rho_e} - \dfrac{N_x \cos\varphi_e \sin\theta_e}{\rho_e} \\ -\dfrac{\sin\varphi_e \sin\theta_e(\upsilon + N_y)}{\rho_e} \\ \Phi_r = q\sin\varphi_e \tan\theta_e - \dfrac{u\sin\varphi_e}{\rho_e\cos\theta_e} \\ -\dfrac{N_x \sin\varphi_e}{\rho_e\cos\theta_e} + \dfrac{\cos\varphi_e(\upsilon + N_y)}{\rho_e\cos\theta_e} \end{cases} \tag{16}$$

C. ASSUMPTIONS AND LEMMAS

Assumption 1: The external disturbances on each degree of freedom are bounded such that $|\bar{f}_n(t)| < \chi_{n\max}, i = u, v, w, q, r$, and $\chi_{n\max}$ represents the unknown positive constants.

Assumption 2 ([38], [40]): In Eqs.(4) and (9), the sway velocity and heave velocity are also bounded and satisfy the following inequalities:

$$\begin{cases} \sup\limits_{t\geq 0} |\upsilon| < \upsilon_a \\ \sup\limits_{t\geq 0} |w| < w_a \end{cases} \tag{17}$$

where υ_a and w_a are unknown constants.

Assumption 3: The three-dimensional expected trajectories and their first and second derivatives, including $x_h, \dot{x}_h, y_h, \dot{y}_h, z_h, \dot{z}_h, \ddot{x}_h, \ddot{y}_h, \ddot{z}_h$, are bounded.

Assumption 4: The pitch angle is bounded due to metacentric restoring forces, and it satisfies $|\Theta| < \frac{\pi}{2}$. Therefore, underwater vehicles cannot approach the neighborhood of $\Theta = +\frac{\pi}{2}$.

Lemma 1 ([46]): $\vartheta_m > 0, m = 1, \ldots\ldots, N$. The following inequalities hold:

$$\begin{cases} \sum\limits_{m=1}^{N} \vartheta_m^r \geq \left(\sum\limits_{m=1}^{N} \vartheta_m\right)^r & \text{if } 0<r \leq 1 \\ \sum\limits_{m=1}^{N} \vartheta_m^r \geq N^{1-r}\left(\sum\limits_{m=1}^{N} \vartheta_m\right)^r & \text{if } 1<r < \infty \end{cases} \tag{18}$$

Lemma 2 ([13]): Assume that an autonomous nonlinear system $\dot{x} = f(x)$ satisfies $\theta > 0, \varsigma < 1$ and $0 < \mathfrak{q} < 1$ such that

$$\dot{V}(x) \leq -\frac{V(x)^{\theta\mathfrak{q}-\theta+1}}{\theta\varsigma(1-\mathfrak{q})T_c}(V(x)^{\theta} + \varsigma)^{2-\mathfrak{q}} + \delta \tag{19}$$

where the predefined time $T_c > 0$ and $\delta \geq 0$ stands for a small positive parameter. According to the literature, System (19) can stabilize for a predefined time T_c.

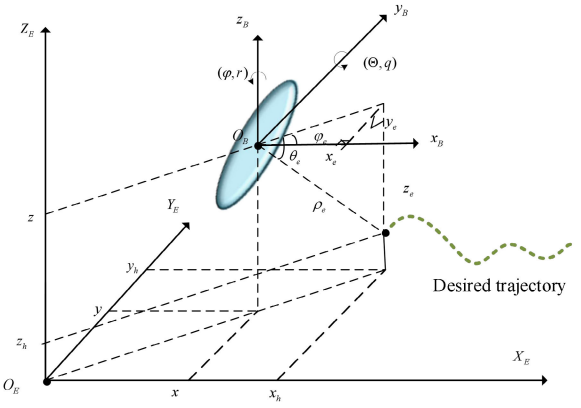

FIGURE 1. AUV frame and coordinates.

Lemma 3 ([47]): In the case of any arbitrary real $\varepsilon > 0, \gamma \in R$, the following inequality holds:

$$0 \leq |\gamma| - \frac{\gamma^2}{\sqrt{\gamma^2 + \varepsilon^2}} \leq \varepsilon \tag{20}$$

Lemma 4: In the case of any actual value a, b, the following inequality holds:

$$ab \leq \frac{1}{2}(a^2 + b^2) \tag{21}$$

III. EVENT-TRIGGERED PREDEFINED-TIME H_∞ CONTROL

The flow chart of the proposed predefined-time H_∞ trajectory tracking control scheme is shown in Fig. 2, and the pseudocode of the algorithm is given in Algorithm 1. As shown in Fig. 2 and Table 1, the position error is obtained by subtracting the AUV model from the desired trajectory, and the LOS error is obtained from the position error. Then, the prescribed performance error is converted, and the auxiliary controller is designed. To reduce the computational complexity, the auxiliary controller is passed through a filter. The predefined-time H_∞ controller can be calculated at this point. To save communication resources, an event-triggered method is introduced. Finally, considering the limited output of the actual actuator, actuator saturation is introduced, and the final derived control force and torque are input into the AUV model to obtain the new position and velocity of the model.

A. SELF-ADJUSTING PRESCRIBED PERFORMANCE CONTROL

The position error ρ_e, pitch angle error θ_e and yaw angle error φ_e satisfy the following prescribed performance conditions:

$$\begin{cases} \rho_e < |\varpi_u| \\ \theta_e < |\varpi_q| \\ \varphi_e < |\varpi_r| \end{cases} \tag{22}$$

where $\varpi_v (v = u, q, r)$ is an improved performance function and is defined as follows:

$$\varpi_v = \frac{sign(\delta_e(0)) + \lambda_{v1}}{\exp(\lambda_{v2}t + \lambda_{v3}) - 1} + \lambda_{v4}\rho_{v\infty} + \kappa_{cv1}\left[\exp(\kappa_{cv2}|\upsilon_{ve}|) - 1\right] \tag{23}$$

TABLE 1. Predefined-time H_∞ controller design.

Algorithm 1	Predefined-time H_∞ controller design
Step 1:	Build the AUV model and provide the initial values
Step 2:	Subtracting the AUV model from the desired trajectory yields the position error x_e, y_e, z_e
Step 3:	LOS conversion yields error $\rho_e, \theta_e, \varphi_e$
Step 4:	Perform the prescribed performance error conversion ξ_ν
Step 5:	Calculate the auxiliary controller and propel the auxiliary controller through the predefined-time filter
Step 6	Calculate the H_∞ controller
Step 7	H_∞ controller saves communication resources after event triggering
Step 8	Set the actuator saturation value

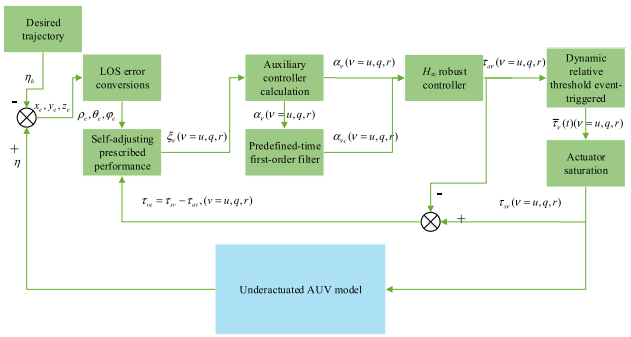

FIGURE 2. Algorithm flowchart.

where $\delta_e = \rho_e, \theta_e, \varphi_e$, and $\delta_e(0)$ is the initial value of the error. The design parameters satisfy $0 < \lambda_{\nu 1} < 1, 0 < \lambda_{\nu 4} < 1$, and $\lambda_{\nu 2} \in R^+, \lambda_{\nu 3} \in R^+, \kappa_{c\nu 1} \in R^+, \kappa_{c\nu 2} \in R^+, \rho_{\nu\infty} \in R^+$. $\upsilon_{\nu e}$ is the error term.

A judgment mechanism is proposed to solve the singularity problem when the actuator is saturated. When the actuator is saturated, the value of the velocity error ν_e is transmitted to the error term υ_e, while when the actuator is not saturated, the error term is zero. Therefore, when the error becomes larger due to actuator saturation, the boundary function can adjust the boundary value according to the magnitude of the error change to prevent the singularity problem caused by a sudden increase in the error beyond the boundary.

The flow graph of this judgment method is shown in Fig. 3.

Remark 2: Traditional prescribed performance functions, such as those in references [6], [9], and [22], are in the form of ordinary time-varying functions. When the actuator is saturated, tracking error mutation likely occurs beyond the performance function boundary, resulting in a singularity problem.

Remark 3: The self-adjusting performance function designed in this paper is an improvement of the function in reference [26]. The performance function in reference [26] is

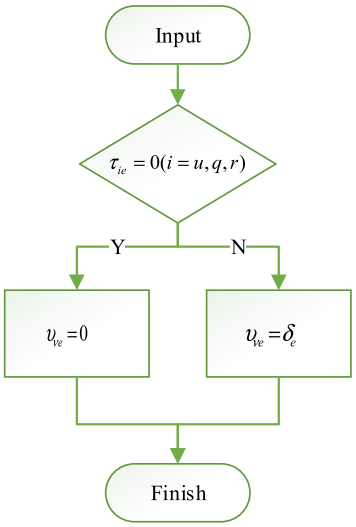

FIGURE 3. Judgment mechanism.

based on $k_1 \left(\exp(k_2 |\tau_{\nu e}|) - 1\right), k_1, k_2 > 0$ to achieve automatic adjustment of the boundary function when the actuator is saturated. However, for an underactuated system, the number of actuators is less than the degrees of freedom of the system, so the initial controlling force or torque of the actuator is generally large, so the saturation of the actuator is also large. If $k_1 \left(\exp(k_2 |\tau_{\nu e}|) - 1\right), k_1, k_2 > 0$ is used in an underactuated system, the boundary function is likely to diverge due to excessive actuator saturation, which leads to system tracking failure. The self-adjusting performance function designed in this paper changes $k_1 \left(\exp(k_2 |\tau_{\nu e}|) - 1\right), k_1, k_2 > 0$ to $\kappa_{c\nu 1} \left[\exp(\kappa_{c\nu 2} |\upsilon_e|) - 1\right]$ and adds the abovementioned judgment mechanism to eliminate this problem.

To transform the error from a constrained state to an unconstrained state, we use the following transition function:

$$\xi_\nu = \frac{\varpi_\nu \delta_e}{\varpi_\nu - \delta_e} \tag{24}$$

where $\delta_e = \rho_e, \theta_e, \varphi_e$ and $\nu = u, q, r$. If and only if $\delta_e = 0$, $\xi_\nu = 0$; furthermore, when $\delta_e \to \varpi_\nu, \xi_\nu \to \infty$. Therefore, if ξ_ν is bounded, the error $\delta_e = \rho_e, \theta_e, \varphi_e$ will not exceed the constraint ϖ_ν. The error can be kept within the prescribed bounds through the selection of the appropriate boundary constraint function and parameters.

Remark 4: Compared with the Ln-type transformation function in references [25] and [26], the proposed transformation function is simpler to calculate and more usable. If $\varpi_\nu \to \infty$, $\lim_{\varpi_\nu \to \infty} \xi_\nu = \delta_e$, which means that the performance function diverges, and the error is not constrained. Therefore, the transition function can be used with or without the error constraint requirement.

B. PREDEFINED-TIME H_∞ CONTROLLER DESIGN

Theorem 1: For the following error dynamics system:

$$\begin{cases} \dot{x} = f(t) + \Im(x)\bar{u} + \phi(x) \\ Z = h(x) \end{cases} \tag{25}$$

where x is the error state variable of the system, $\bar{u}$ indicates the control input to be designed, $f(t)$ is the uncertainty interference, $\Im(x)$ and $\phi(x)$ are system functions, and $h(x)$ is the performance metric vector.

Defining a position number $\Upsilon > 0$, the system has an L_2 gain that is less than Υ if for all $f \in L_2[t_0, t_1]$ with $t_1 > t_0$,

$$\int_{t_0}^{t_1} \|Z(t)\|^2 dt \leq \Upsilon^2 \int_{t_0}^{t_1} \|f(t)\|^2 dt \tag{26}$$

For system (25), assume that there exists a Lyapunov function $V(x)$ in an origin field $\hat{U}_0 \subset R^n$. An H_∞ controller $\bar{u}$ (also called a causal dynamic compensator) is designed by setting an appropriate value of Υ; if the controller can make the system satisfy the elements described in Lemma 2 and the following two conditions, it can be named a predefined-time H_∞ controller.

(1) $V(x)$ is a positive definite function within $\hat{U}_0$.

(2) $\dot{V}(x) + \frac{V(x)^{\theta\phi-\theta+1}}{\varsigma\theta(1-\phi)T_c}(V(x)^\theta + \varsigma)^{2-\phi} - \delta \leq \frac{1}{2}(\Upsilon^2 \|f\|^2 - \|Z\|^2)$

where $0 < \theta, \varsigma > 1$, $1 < \phi < 0$ and $T_c > 0$. $\delta \geq 0$ represents a small positive parameter. Then, Eq. (25) is locally predefined-time stable, and the gain of the system is less than or equal to Υ. The origin of Eq. (25) is predefined-time stable if $\hat{U}_0 = R^n$ and $V(x)$ are radially unbounded.

Proof.

If $f(t) = 0$, Condition (2) in Theorem 1 can be written as:

$$\dot{V}(x) + \frac{V(x)^{\theta\phi-\theta+1}}{\varsigma\theta(1-\phi)T_c}(V(x)^\theta + \varsigma)^{2-\phi} - \delta \leq -\|Z\|^2 \tag{27}$$

According to Lemma 2, system (25) is predefined-time stable.

If $f(t) \neq 0$, it can be deduced that:

$$\begin{aligned}\dot{V}(x) &\leq \dot{V}(x) + \frac{V(x)^{\theta\phi-\theta+1}}{\varsigma\theta(1-\phi)T_c}(V(x)^\theta + \varsigma)^{2-\phi} - \delta \\ &\leq \frac{1}{2}(\Upsilon^2 \|f\|^2 - \|Z\|^2)\end{aligned} \tag{28}$$

According to (26), the L_2 gain of system (25) is less than or equal to Υ. Thus, Eq. (25) is locally predefined-time stable, and the gain of the system is less than or equal to Υ. The proof of Theorem 1 is complete.

In the AUV trajectory tracking control system, the main errors are the position error, angle error and velocity error. However, this paper uses the LOS method to convert the position and angle errors $x_e, y_e, z_e, \Theta_e, \varphi_e$ to the LOS error $\delta_e = \rho_e, \theta_e, \varphi_e$. To better constrain the error and introduce the preset performance method, the LOS error $\delta_e = \rho_e, \theta_e, \varphi_e$ is converted to $\xi_\nu (\nu = u, q, r)$ again. Therefore, the error variable of the system should be $\xi_\nu (\nu = u, q, r)$, and the velocity error should be $\nu_e = \nu - \alpha_\nu (\nu = u, q, r)$.

Combining Eq. (14) and the above errors yields:

$$\begin{aligned}\dot{\xi}_\nu &= \Gamma_\nu(\varpi_\nu^2 \dot{\delta}_e + \delta_e^2 \dot{\varpi}_\nu) \\ &= \Gamma_\nu(\varpi_\nu^2(\nu L_\nu + Q_\nu) + \delta_e^2 \dot{\varpi}_\nu)\end{aligned} \tag{29}$$

$$\Gamma_\nu = \frac{1}{(\varpi_\nu - \delta_e)^2} \tag{30}$$

Combining Eq. (9) with the derivation of the velocity error yields:

$$\begin{aligned}\dot{\nu}_e &= \dot{\nu} - \dot{\alpha}_\nu \\ &= P_\nu + T_\nu \tau_{a\nu} + f_\nu - \dot{\alpha}_\nu\end{aligned} \tag{31}$$

Z is the performance vector with adjustable parameters related to the system error vector. The performance metric vector is selected as follows:

$$Z = \begin{bmatrix} \lambda_1 \xi_\delta \\ \lambda_2 \nu_e \end{bmatrix} \tag{32}$$

According to Eq. (29), Eq. (31) and Eq. (32), the following underactuated AUV error dynamics system can be established:

$$\begin{cases} \dot{\xi}_\delta = \nu_e \varpi_\nu^2 \Gamma_\nu L_\nu + \alpha_\nu \varpi_\nu^2 \Gamma_\nu L_\nu - \dot{\varpi}_\nu \Gamma_\nu \delta_e^2 \\ \dot{\nu}_e = P_\nu + T_\nu \tau_{a\nu} + f_\nu - \dot{\alpha}_\nu \\ Z = \begin{bmatrix} \lambda_1 \xi_\delta \\ \lambda_2 \nu_e \end{bmatrix} \end{cases} \tag{33}$$

where $\tau_{a\nu} (\nu = u, q, r)$ indicates the controller to be designed and $f_\nu (\nu = u, q, r)$ is the uncertain interference. α_ν is the auxiliary controller.

The following Lyapunov function is designed:

$$V_1 = \frac{1}{2}\xi_\nu^2 \tag{34}$$

where $\nu = u, q, r$. Combining the error system (33) and Eq.(34) yields:

$$\begin{aligned}\dot{V}_1 &= \xi_\nu \dot{\xi}_\nu \\ &= \xi_\nu \Gamma_\nu \varpi_\nu^2 L_\nu \nu_e + \Gamma_\nu \xi_\nu (\varpi_\nu^2 (Q_\nu + \alpha_\nu L_\nu) + \delta_e^2 \dot{\varpi}_\nu)\end{aligned} \tag{35}$$

where α_ν is the auxiliary controller.

Then, the auxiliary controller is designed as follows:

$$\alpha_\nu = L_\nu^{-1} \left(\begin{pmatrix} -Q_\nu \\ -\varpi_\nu^{-2} \end{pmatrix} \begin{pmatrix} \delta_e^2 \dot{\varpi}_\nu \\ + \frac{\Gamma_\nu^{-1} 2^{\theta-\theta\phi-1}}{\theta\varsigma(1-\phi)T_c} \begin{pmatrix} sig\,(\xi_\nu)^{2\theta\phi-2\theta+1} \cdot \\ (\frac{|\xi_\nu|^{2\theta}}{2^\theta} + \varsigma)^{2-\phi} \end{pmatrix} \\ + \ell \Gamma_\nu^{-1} \xi_\nu \end{pmatrix} \right) \tag{36}$$

where $\ell > 0$ is the controller parameter.

Remark 5: The expression $sig(x)^y = |x|^y sign(x)$.

Substituting Eq. (36) into Eq. (35) yields:

$$\begin{aligned}\dot{V}_1 &= \Gamma_\nu \xi_\nu \varpi_\nu^2 \nu_e L_\nu + \Gamma_\nu \xi_\nu (\varpi_\nu^2 (\alpha_\nu L_\nu + Q_\nu) + \delta_e^2 \dot{\varpi}_\nu) \\ &= \Gamma_\delta \xi_\delta \varpi_\nu^2 \nu_e L_\nu \\ &\quad + \Gamma_\nu \xi_\nu (-\frac{\Gamma_\nu^{-1} 2^{\theta-\theta\phi-1}}{\varsigma\theta(1-\phi)T_c} sig\,(\xi_\nu)^{2\theta\phi-2\theta+1} (\frac{|\xi_\nu|^{2\theta}}{2^\theta} + \varsigma)^{2-\phi} \\ &\quad - \ell \xi_\nu \Gamma_\nu^{-1}) \\ &= \Gamma_\nu \xi_\nu \varpi_\nu^2 \nu_e L_\nu \\ &\quad - \frac{2^{\theta-\theta\phi-1}}{\varsigma\theta(1-\phi)T_c} sig\,(\xi_\nu)^{2\theta\phi-2\theta+2} (\frac{|\xi_\nu|^{2\theta}}{2^\theta} + \varsigma)^{2-\phi} \\ &\quad - \ell \xi_\nu^2\end{aligned} \tag{37}$$

To solve the "differential explosion" problem, a predefined-time first-order filter is designed as follows:

$$\kappa_{vc}\dot{\alpha}_{vc} + \alpha_{vc} = \alpha_{nvc}, \alpha_{vc}(0) = \alpha_{nvc}(0) \tag{38}$$

$$\alpha_{nvc} = \kappa_{vc}\frac{2^{\theta-\theta q-1}}{\theta\varsigma(1-q)T_c} sig\,(e_{vc})^{2\theta q-2\theta+1} \cdot (\frac{1}{2^{\theta}}\|e_{vc}\|^{2\theta} + \varsigma)^{2-q} + \alpha_{v} \tag{39}$$

where α_v and α_{vc} represent the auxiliary controller and the filtered auxiliary controller, respectively. $\kappa_{vc} > 0$ is the filtering parameter, and the error between them is defined as follows:

$$e_{vc} = \alpha_v - \alpha_{vc} \tag{40}$$

We further design the Lyapunov function as follows:

$$V_2 = V_1 + \frac{1}{2}e_{vc}^2 + \frac{1}{2}\nu_e^2 \tag{41}$$

Derivation of Eq.(41) and combining it with Eq. (37), Eq. (38), Eq. (39) and Eq. (40), Eq. (33) yields:

$$\begin{aligned}\dot{V}_2 = {} & \Gamma_v\xi_v\varpi_v^2\nu_e L_v \\ & - \frac{2^{\theta-\theta q-1}}{\theta\varsigma(1-q)T_c} sig\,(\xi_v)^{2\theta q-2\theta+2}(\frac{1}{2^{\theta}}|\xi_v|^{2\theta} + \varsigma)^{2-q} \\ & - \ell\xi_v^2 + e_{vc}\dot{\alpha}_v \\ & - \frac{2^{\theta-\theta q-1}}{\theta\varsigma(1-q)T_c} sig\,(e_{vc})^{2\theta q-2\theta+2}(\frac{|e_{vc}|^{2\theta}}{2^{\theta}} + \varsigma)^{2-q} \\ & + \nu_e(P_v + T_v\tau_{av} + f_v - \dot{\alpha}_{vc})\end{aligned} \tag{42}$$

$$\begin{cases} P_u = \dfrac{m_{22}}{m_{11}}vr - \dfrac{m_{33}}{m_{11}}qw - \dfrac{d_{11}}{m_{11}}u \\ P_q = \dfrac{(m_{33}-m_{11})}{m_{55}}uw - \dfrac{d_{55}}{m_{55}}q - \dfrac{\rho g\overline{GM_L}\sin\theta}{m_{55}} \\ P_r = \dfrac{(m_{11}-m_{22})}{m_{66}}vu - \dfrac{d_{66}}{m_{66}}r \end{cases} \tag{43}$$

$$\begin{cases} T_u = \dfrac{1}{m_{11}} \\ T_q = \dfrac{1}{m_{55}} \\ T_r = \dfrac{1}{m_{66}} \end{cases} \tag{44}$$

For the purpose of designing the H_∞ robust controller, Y_v is defined as:

$$Y_v = \dot{V}_2 + \frac{1}{2}(\|Z\|^2 - \Upsilon^2\|f_v\|^2) \tag{45}$$

By combining Eq. (42) and Eq. (33), Eq. (45) can be rewritten as:

$$\begin{aligned}Y_v = {} & \dot{V}_2 + \frac{1}{2}(\lambda_1^2\xi_v^2 + \lambda_2^2\nu_e^2 - \Upsilon^2\|f_v\|^2) \\ = {} & \Gamma_v\xi_v\varpi_v^2\nu_e L_v \\ & - \frac{2^{\theta-\theta q-1}}{\theta\varsigma(1-q)T_c} sig\,(\xi_v)^{2\theta q-2\theta+2}(\frac{1}{2^{\theta}}|\xi_v|^{2\theta} + \varsigma)^{2-q} \\ & - \ell\xi_v^2 + e_{vc}\dot{\alpha}_v \\ & - \frac{2^{\theta-\theta q-1}}{\theta\varsigma(1-q)T_c} sig\,(e_{vc})^{2\theta q-2\theta+2}(\frac{1}{2^{\theta}}|e_{vc}|^{2\theta} + \varsigma)^{2-q} \\ & + \nu_e(P_v + T_v\tau_{av} - \dot{\alpha}_{vc}) \\ & + \frac{1}{2}\lambda_1^2\xi_v^2 + \frac{1}{2}\lambda_2^2\nu_e^2 - \frac{1}{2}\Upsilon^2\|f_v\|^2 + \nu_e f_v\end{aligned} \tag{46}$$

The H_∞ predefined-time controller is designed on the basis of Eq. (46) as follows:

$$\begin{aligned}\tau_{av} = {} & T_v^{-1}(\dot{\alpha}_{vc} - P_v - \Gamma_v\xi_v\varpi_v^2 L_v \\ & - \frac{1}{2}\lambda_2^2\nu_e - \frac{1}{2\Upsilon^2}\nu_e \\ & - \frac{2^{\theta-\theta q-1}}{\theta\varsigma(1-q)T_c} sig\,(\nu_e)^{2\theta q-2\theta+1}(\frac{1}{2^{\theta}}|\nu_e|^{2\theta} + \varsigma)^{2-q})\end{aligned} \tag{47}$$

C. DYNAMIC-RELATIVE THRESHOLD EVENT-TRIGGERED MECHANISM

The dynamic relative threshold event-triggered mechanism is designed to provide a less frequent control signal (Eq.(6)) transmission as a way to save communication resources. The dynamic event-triggered adaptive controller is designed in conjunction with Eq. (47) as follows:

$$n_v(t) = -(1+\mu_v)(\frac{\nu_e\tau_{av}^2}{\sqrt{\nu_e^2\tau_{av}^2 + \varepsilon_v^2}} + \frac{\nu_e\bar{j}_v^2}{\sqrt{\nu_e^2\bar{j}_v^2 + \varepsilon_v^2}}) \tag{48}$$

$$\bar{\tau}_v(t) = n_v(t_i), \forall t \in [t_i, t_{i+1}) \tag{49}$$

$$t_{i+1} = \inf\{t \in R|\,|e_{\tau v}(t)| \geq \mu_v\,|n_v(t)| + j_v\} \tag{50}$$

where $0 < \mu_v < 1, j_v > 0, \bar{j}_v > \frac{j_v}{1-\mu_v}$ and $v = u, q, r$. The error generated by the event trigger is expressed as $e_{\tau v}(t) = n_v(t) - \bar{\tau}_v$. The adaptive dynamic parameters μ_v are defined as follows:

$$\dot{\mu}_v = -d_{\mu_v}\mu_v^2 \tag{51}$$

where $d_{\mu_v} > 0$.

Remark 6: For an underactuated AUV error dynamics system (33), by replacing the saturated controller in (6) with the event-triggered controller in (49), the relevant properties in Theorem 1 still hold. The proof is given in Section IV.

Remark 7: Different from the event-triggered controller in [33], the proposed event-triggered controller is derived from Lemma 3 and provides an alternative solution to dynamic threshold event-triggered control.

Remark 8: Since the underactuated AUV trajectory tracking control system starts with a relatively large control force and torques, a smaller time trigger interval is used. After reaching a predefined stabilization time, most of the time, the forces and torques are smaller than the saturation forces or torques, so using a smaller event trigger interval can lead to better controller performance.

IV. PREDEFINED-TIME STABILITY ANALYSIS

For the trajectory tracking control of the underactuated AUV with external uncertain disturbances and actuator saturation, if the initial error is bounded, all the assumptions are valid.

When the error is always within the prescribed boundary range and converges to the neighborhood of zero within a predefined time, we can conclude that all the signals in the closed-loop system are guaranteed to be uniform and eventually limited.

In this section, three stages are divided, including the controller stage without event-trigger stability analysis, the event-triggered controller stability analysis stage and the final stage, which proves that no zeno behavior exists.

A. CONTROLLER WITHOUT EVENT-TRIGGER STABILITY ANALYSIS

According to Eq. (47), Eq. (46) can be written as:

$$\begin{aligned}
Y_v =& -\frac{2^{\theta-\theta q-1}}{\theta\varsigma(1-q)T_c} sig\,(\xi_v)^{2\theta q-2\theta+2}\left(\frac{1}{2^\theta}|\xi_v|^{2\theta}+\varsigma\right)^{2-q} \\
&-\ell\xi_v^2-\frac{1}{2}\lambda_2^2 v_e^2-\frac{1}{2\Upsilon^2}v_e^2 \\
&-\frac{2^{\theta-\theta q-1}}{\theta\varsigma(1-q)T_c} sig\,(v_e)^{2\theta q-2\theta+2}\left(\frac{1}{2^\theta}|v_e|^{2\theta}+\varsigma\right)^{2-q} \\
&-\frac{2^{\theta-\theta q-1}}{\theta\varsigma(1-q)T_c} sig\,(e_{vc})^{2\theta q-2\theta+2}\left(\frac{1}{2^\theta}|e_{vc}|^{2\theta}+\varsigma\right)^{2-q} \\
&+e_{vc}\dot{\alpha}_v+\frac{1}{2}\lambda_1^2\xi_v^2+\frac{1}{2}\lambda_2^2 v_e^2-\frac{1}{2}\Upsilon^2\|f_v\|^2+v_e f_v \\
=& -\frac{2^{\theta-\theta q-1}}{\theta\varsigma(1-q)T_c} sig\,(\xi_v)^{2\theta q-2\theta+2}\left(\frac{1}{2^\theta}|\xi_v|^{2\theta}+\varsigma\right)^{2-q} \\
&-\frac{2^{\theta-\theta q-1}}{\theta\varsigma(1-q)T_c} sig\,(v_e)^{2\theta q-2\theta+2}\left(\frac{1}{2^\theta}|v_e|^{2\theta}+\varsigma\right)^{2-q} \\
&-\frac{2^{\theta-\theta q-1}}{\theta\varsigma(1-q)T_c} sig\,(e_{vc})^{2\theta q-2\theta+2}\left(\frac{1}{2^\theta}|e_{vc}|^{2\theta}+\varsigma\right)^{2-q} \\
&+e_{vc}\dot{\alpha}_v+\frac{1}{2}\lambda_1^2\xi_v^2-\ell\xi_v^2-\frac{1}{2\Upsilon^2}v_e^2-\frac{1}{2}\Upsilon^2\|f_v\|^2+v_e f_v \\
\le& -\frac{2^{\theta-\theta q-1}}{\theta\varsigma(1-q)T_c} sig\,(\xi_v)^{2\theta q-2\theta+2}\left(\frac{1}{2^\theta}|\xi_v|^{2\theta}+\varsigma\right)^{2-q} \\
&-\frac{2^{\theta-\theta q-1}}{\theta\varsigma(1-q)T_c} sig\,(v_e)^{2\theta q-2\theta+2}\left(\frac{1}{2^\theta}|v_e|^{2\theta}+\varsigma\right)^{2-q} \\
&-\frac{2^{\theta-\theta q-1}}{\theta\varsigma(1-q)T_c} sig\,(e_{vc})^{2\theta q-2\theta+2}\left(\frac{1}{2^\theta}|e_{vc}|^{2\theta}+\varsigma\right)^{2-q} \\
&+e_{vc}\dot{\alpha}_v-(\ell-\frac{1}{2}\lambda_1^2)\xi_v^2 \qquad (52)
\end{aligned}$$

When $\ell \ge \frac{1}{2}\lambda_1^2$, combining Lemma 1 and Lemma 4, Eq. (52) can be updated to:

$$\begin{aligned}
Y_v \le& -\frac{1}{\theta\varsigma(1-q)T_c} sig\left(\frac{\xi_v^2}{2}\right)^{\theta q-\theta+1}\left(\left(\frac{\xi_v^2}{2}\right)^{\theta}+\varsigma\right)^{2-q} \\
&-\frac{1}{\theta\varsigma(1-q)T_c} sig\left(\frac{v_e^2}{2}\right)^{\theta q-\theta+1}\left(\left(\frac{v_e^2}{2}\right)^{\theta}+\varsigma\right)^{2-q} \\
&-\frac{1}{\theta\varsigma(1-q)T_c} sig\left(\frac{e_{vc}^2}{2}\right)^{\theta q-\theta+1}\left(\left(\frac{e_{vc}^2}{2}\right)^{\theta}+\varsigma\right)^{2-q}+\partial \\
=& -\frac{sig\,(V_2)^{\theta q-\theta+1}}{\theta\varsigma(1-q)T_c}(V_2^\theta+\varsigma)^{2-q}+\partial \qquad (53)
\end{aligned}$$

where $\partial = |e_{vc}\dot{\alpha}_v| \ge 0$.

In summary, the following can be obtained:

$$\begin{aligned}
Y_v =& \dot{V}_2+\frac{1}{2}(\|z\|^2-\Upsilon^2\|f_v\|^2) \\
\le& -\frac{sig\,(V_2)^{\theta q-\theta+1}}{\theta\varsigma(1-q)T_c}(V_2^\theta+\varsigma)^{2-q}+\partial \qquad (54)
\end{aligned}$$

Eq. (54) can be written as:

$$\begin{aligned}
&\dot{V}_2+\frac{V_2^{\theta q-\theta+1}}{\theta\varsigma(1-q)T_c}(V_2^\theta+\varsigma)^{2-q}-\partial \\
&\le \frac{1}{2}(\Upsilon^2\|f_v\|^2-\|z\|^2) \qquad (55)
\end{aligned}$$

According to Lemma 5, the proposed H_∞ controller is predefined-time stable within the prescribed time T_c.

B. EVENT-TRIGGERED CONTROLLER STABILITY ANALYSIS

Eq. (50) in the interval $[t_i, t_{i+1})$ is transformed into $n_v(t) = (1+\kappa_{v1}(t)\mu_v)\bar{\tau}_v + \kappa_{v2}(t)j_v$ with time-varying parameters $|\kappa_{v1}| \le 1$ and $|\kappa_{v2}| \le 1$. Therefore, we can obtain

$$\bar{\tau}_v = \frac{n_v(t)-\kappa_{v2}(t)j_v}{1+\kappa_{v1}(t)\mu_v} \qquad (56)$$

According to Remark 1, the controller saturation after event triggering is expressed as $\bar{\tau}_{va}(v = u, q, r)$, and the actuator saturation value in Eq. (8) changes to $\tau_{ve} = \bar{\tau}_{va} - \bar{\tau}_v$.

Substituting Eq. (56) instead of τ_{av} into Eq. (46) yields:

$$\begin{aligned}
Y_v =& \Gamma_v\xi_v\varpi_v^2 v_e L_v \\
&-\frac{2^{\theta-\theta q-1}}{\theta\varsigma(1-q)T_c} sig\,(\xi_v)^{2\theta q-2\theta+2}\left(\frac{1}{2^\theta}|\xi_v|^{2\theta}+\varsigma\right)^{2-q}-\ell\xi_v^2 \\
&-\frac{2^{\theta-\theta q-1}}{\theta\varsigma(1-q)T_c} sig\,(e_{vc})^{2\theta q-2\theta+2}\left(\frac{1}{2^\theta}|e_{vc}|^{2\theta}+\varsigma\right)^{2-q} \\
&+\frac{1}{2}\lambda_1^2\xi_v^2+\frac{1}{2}\lambda_2^2 v_e^2-\frac{1}{2}\Upsilon^2\|f_v\|^2+v_e f_v+e_{vc}\dot{\alpha}_v \\
&+v_e\left(P_v+T_v\left(\frac{n_v(t)-\kappa_{v2}(t)j_v}{1+\kappa_{v1}(t)\mu_v}\right)-\dot{\alpha}_{vc}\right) \qquad (57)
\end{aligned}$$

Because $\left|\frac{\kappa_{v2}(t)j_v}{1+\kappa_{v1}(t)\mu_v}\right| \le \frac{j_v}{1-\mu_v}$ and $\frac{n_v(t)}{1+\kappa_{v1}(t)\mu_v} \le \frac{n_v(t)}{1+\mu_v}$, Eq. (57) can be written as:

$$\begin{aligned}
Y_v \le& \Gamma_v\xi_v\varpi_v^2 v_e L_v \\
&-\frac{2^{\theta-\theta q-1}}{\theta\varsigma(1-q)T_c} sig\,(\xi_v)^{2\theta q-2\theta+2}\left(\frac{1}{2^\theta}|\xi_v|^{2\theta}+\varsigma\right)^{2-q} \\
&-\ell\xi_v^2+e_{vc}\dot{\alpha}_v \\
&-\frac{2^{\theta-\theta q-1}}{\theta\varsigma(1-q)T_c} sig\,(e_{vc})^{2\theta q-2\theta+2}\left(\frac{1}{2^\theta}|e_{vc}|^{2\theta}+\varsigma\right)^{2-q} \\
&+\frac{1}{2}\lambda_1^2\xi_v^2+\frac{1}{2}\lambda_2^2 v_e^2-\frac{1}{2}\Upsilon^2\|f_v\|^2+v_e f_v \\
&+v_e\left(P_v+T_v\left(\begin{array}{l}-\left(\frac{v_e\tau_v^2}{\sqrt{v_e^2\tau_v^2+\varepsilon_v^2}}\right.\\ \left.+\frac{v_e j_v^2}{\sqrt{v_e^2 j_v^2+\varepsilon_v^2}}\right)\\ +\left|\frac{\kappa_{v2}(t)j_v}{1-\mu_v}\right|\end{array}\right)-\dot{\alpha}_{vc}\right) \qquad (58)
\end{aligned}$$

From Lemma 3, Eq. (58) is updated as follows:

$$
\begin{aligned}
Y_v \le\ & \Gamma_v \xi_v \varpi_v^2 \nu_e L_v \\
& - \frac{2^{\theta-\theta\varphi-1}}{\theta\varsigma(1-\varphi)T_c} sig\,(\xi_v)^{2\theta\varphi-2\theta+2} \left(\frac{1}{2^\theta}\,|\xi_v|^{2\theta}+\varsigma\right)^{2-\varphi} \\
& - \ell\xi_v^2 + e_{vc}\dot{\alpha}_v \\
& - \frac{2^{\theta-\theta\varphi-1}}{\theta\varsigma(1-\varphi)T_c} sig\,(e_{vc})^{2\theta\varphi-2\theta+2} \left(\frac{1}{2^\theta}\,|e_{vc}|^{2\theta}+\varsigma\right)^{2-\varphi} \\
& + \frac{1}{2}\lambda_1^2\xi_v^2 + \frac{1}{2}\lambda_2^2\nu_e^2 - \frac{1}{2}\Upsilon^2\|f_v\|^2 + \nu_e f_v \\
& + P_v\nu_e + T_v\left(-(|\nu_e\tau_v| + |\nu_e\bar{j}_v|) + 2\varepsilon_v + \left|\frac{\nu_e j_v}{1-\mu_v}\right|\right) \\
& - \nu_e\dot{\alpha}_{vc} \\
\le\ & \Gamma_v \xi_v \varpi_v^2 \nu_e L_v \\
& - \frac{2^{\theta-\theta\varphi-1}}{\theta\varsigma(1-\varphi)T_c} sig\,(\xi_v)^{2\theta\varphi-2\theta+2} \left(\frac{1}{2^\theta}\,|\xi_v|^{2\theta}+\varsigma\right)^{2-\varphi} - \ell\xi_v^2 \\
& + e_{vc}\dot{\alpha}_v - \frac{2^{\theta-\theta\varphi-1}}{\theta\varsigma(1-\varphi)T_c} sig\,(e_{vc})^{2\theta\varphi-2\theta+2} \\
& \times \left(\frac{1}{2^\theta}\,|e_{vc}|^{2\theta}+\varsigma\right)^{2-\varphi} \\
& + \frac{1}{2}\lambda_1^2\xi_v^2 + \frac{1}{2}\lambda_2^2\nu_e^2 - \frac{1}{2}\Upsilon^2\|f_v\|^2 + \nu_e f_v \\
& - T_v\,|\nu_e\tau_v| + 2\varepsilon_v T_v - \nu_e\dot{\alpha}_{vc}
\end{aligned}
\tag{59}
$$

Similar to Eq. (52)- Eq. (55), Eq. (59) can be written as:

$$
\dot{V}_2 + \frac{V_2^{\theta\varphi-\theta+1}}{\theta\varsigma(1-\varphi)T_c}(V_2^\theta+\varsigma)^{2-\varphi} - \bar{\partial} \le \frac{1}{2}(\Upsilon^2\|f_v\|^2 - \|z\|^2) \tag{60}
$$

where $\bar{\partial} = \partial + |2\varepsilon_v T_v| \ge 0$ is a small positive parameter.

According to Lemma 4, the proposed H_∞ controller is predefined-time stable within a prescribed time.

C. ZENO BEHAVIOR ANALYSIS

By differentiating the errors of event triggering, we can obtain:

$$
\begin{aligned}
\frac{d}{dt}|e_{\tau\upsilon}(t)| &= \frac{d}{dt}(e_{\tau\upsilon}(t)\times e_{\tau\upsilon}(t))^{\frac{1}{2}} \\
&= sign(e_{\tau\upsilon}(t))\dot{e}_{\tau\upsilon}(t) \le |\dot{n}_v|
\end{aligned}
\tag{61}
$$

The differentiation of n_v is obtained:

$$
\begin{aligned}
\dot{n}_v = {} & d_{\mu_v}\mu_v^2\left(\frac{\nu_e\tau_v^2}{\sqrt{\nu_e^2\tau_v^2+\varepsilon_v^2}} + \frac{\nu_e\bar{j}_v^2}{\sqrt{\nu_e^2\bar{j}_v^2+\varepsilon_v^2}}\right) \\
& - (1+\mu_v)\begin{pmatrix} \frac{\dot{\nu}_e\tau_v^2}{\sqrt{\nu_e^2\tau_v^2+\varepsilon_v^2}} \\ +\nu_e\begin{pmatrix} \frac{2\dot{\tau}_v\tau_v\sqrt{\varepsilon_v^2+\nu_e^2\tau_v^2}}{\nu_e^2\tau_v^2+\varepsilon_v^2} \\ -\frac{\tau_v\nu_e\dot{\nu}_e^2+\nu_e^2\tau_v\dot{\tau}_v}{\sqrt{\varepsilon_v^2+\nu_e^2\tau_v^2}}\tau_v^2 \\ \nu_e^2\tau_v^2+\varepsilon_v^2 \end{pmatrix} \end{pmatrix} \\
& + \frac{\dot{\nu}_e\bar{j}_v^2}{\sqrt{\nu_e^2\bar{j}_v^2+\varepsilon_v^2}} + \nu_e\begin{pmatrix} -\frac{\bar{j}_v\bar{j}_v^2\nu_e\dot{\nu}_e}{\sqrt{\nu_e^2\bar{j}_v^2+\varepsilon_v^2}} \\ \nu_e^2\bar{j}_v^2+\varepsilon_v^2 \end{pmatrix}
\end{aligned}
\tag{62}
$$

Therefore, $\dot{n}_v$ is a bounded and continuous function, and there exists a positive real number such that $|\dot{n}_v| \le n_0$. Here, t_l is defined as the lower bound of the interexecution intervals $\{t_{i+1}-t_i\}$. From Eq. $\lim_{t\to t_{i+1}} e_{\tau\upsilon}(t) = \varepsilon_v|\bar{\tau}_v| + j_v, \forall t \in [t_i, t_{i+1})$ (49) and Eq.(50), $e_{\tau\upsilon}(t_i) = 0$, and. The derivatives are $\dot{e}_{\tau\upsilon}(t) = \lim_{t\to t_{i+1}} \frac{e_{\tau\upsilon}(t)}{t-t_i} = \lim_{t\to t_{i+1}} \frac{\varepsilon_v|\bar{\tau}_v|+j_v}{t-t_i}$ and $\varepsilon_v|\bar{\tau}_v| + j_v \le t_l n_v$. Thus, $t_{i+1} - t_i \ge t_l \ge \frac{\varepsilon_v|\bar{\tau}_v|+j_v}{n_0} > 0$ is established for $\forall t \in [t_i, t_{i+1})$.

In summary, Zeno behavior does not exist in this paper.

V. SIMULATIONS

A simulation of the underactuated AUV is provided to demonstrate the robustness and effectiveness of the proposed control method. The model data in Table 2 are consistent with those in the literature [39], and Table 3 shows the controller data of the underactuated AUV system:.

The initial states are given as $[x_0, y_0, z_0, \Theta_0, \varphi_0, u_0, v_0, w_0, q_0, r_0] = [1.5\ 9.5\ 9.5\ 0\ 0\ 0\ 0\ 0\ 0\ 0]$, and the reference trajectory is obtained from the following options:

$$
\begin{aligned}
& x_h = 10\sin(0.04t),\ y_h = 10\cos(0.02t), \\
& z_h = \sin(0.02t) + 10\cos(0.02t).
\end{aligned}
$$

The simulations and analysis are summarized as follows:

Figs. 4 to 6 show the effectiveness of the proposed predefined-time control method compared with the fixed-time control method proposed in reference [15] and another form of the predefined-time method proposed in reference [32] for trajectory tracking in an underactuated AUV system with the same external disturbances and actuator saturation. The external disturbances and saturation values are chosen as:

$$
\begin{cases}
\omega_u = 3 + 0.3\cos t\cos(0.4t) - 0.3(0.3t)\cos(0.8t) \\
\omega_v = 0.04\cos(0.1t) \\
\omega_w = 0.04\sin(0.1t) \\
\omega_q = 2\sin(0.8t)\cos(0.2t) \\
\omega_r = 2\sin(0.6t)\cos(0.4t)
\end{cases},
$$

$$
\begin{cases}
\tau_{su} = 200N \\
\tau_{sq} = 240N\cdot m \\
\tau_{sr} = 240N\cdot m
\end{cases}.
$$

Fig. 4 represents the 3D simulation results of the trajectory tracking of the proposed predefined-time H_∞ control method, the fixed-time H_∞ control method proposed in Reference 1 [15], and the predefined-time control method proposed in Reference 2 [32] for the underactuated AUV model with external uncertain disturbances and actuator saturation. According to the enlarged figure, the proposed method can track the desired trajectory faster than the methods in Reference 1 and Reference 2. Fig. 5 presents the tracking results of the system in each of the three coordinate axes as an expansion of Fig. 4. It is obvious from Fig. 5 that

TABLE 2. Model data of the underactuated AUV system.

Parameter	Value	Parameter	Value
$m_{11}(kg)$	25.00	$d_{11}(kg\cdot s^{-1})$	30.00
$m_{22}(kg)$	17.50	$d_{22}(kg\cdot s^{-1})$	30.00
$m_{33}(kg)$	30.00	$d_{33}(kg\cdot s^{-1})$	30.00
$m_{55}(kg\cdot m^2)$	22.50	$d_{55}(kg\cdot s^{-1})$	20.00
$m_{66}(kg\cdot m^2)$	15.00	$d_{66}(kg\cdot s^{-1})$	20.00
$\rho g\Delta\overline{GM}_L$	5.00	$\Delta_{d,j}$, $\Delta_{m,j}(j=1,2,3,5,6)$ Δ_g	0.1

TABLE 3. Controller data of the underactuated AUV system.

Parameter	Value	Parameter	Value
λ_{u1}	0.50	λ_{q1}	0.85
λ_{u2}	0.90	λ_{q2}	0.45
λ_{u3}	0.05	λ_{q3}	0.05
λ_{u4}	0.55	λ_{q4}	0.55
$\rho_{u\infty}$	0.68	$\rho_{q\infty}$	0.68
κ_{cu1}	0.80	κ_{cq1}	0.80
κ_{cu2}	3.00	κ_{cq2}	3.00
κ_{uc}	0.10	κ_{qc}	0.10
θ	0.90	q	0.65
T_c	5.00	1	1.00
λ_2	1.00		
$\mu_u(0)$	0.02	$\mu_q(0)$	0.02
j_u	2.50	j_q	10.50
$\overline{j}_u$	12.50	$\overline{j}_q$	20.50
ε_u	3.00	ε_q	3.00

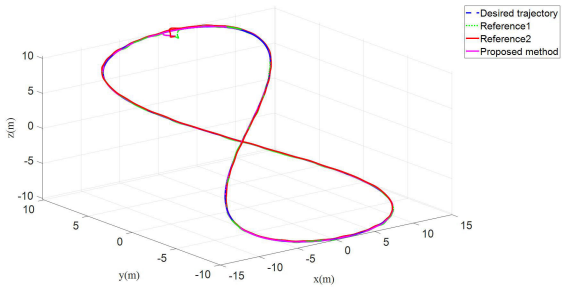

FIGURE 4. 3D trajectory tracking.

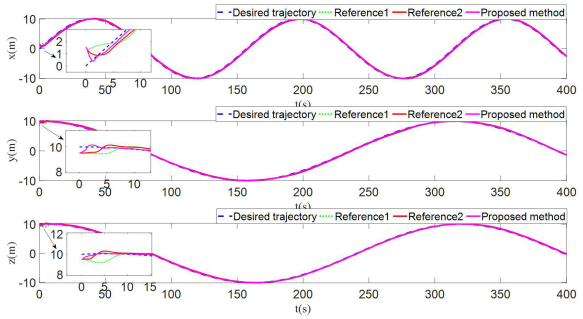

FIGURE 5. Three-directional trajectory tracking.

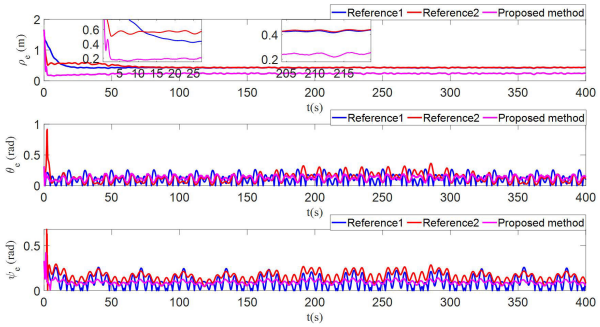

FIGURE 6. Error performance comparison.

TABLE 4. Mean values of the underactuated AUV system tracking errors.

Error	Reference 1	Reference 2	Proposed method
ρ_e (m)	0.491245	0.452740	0.236180
θ_e (rad)	0.345309	0.125720	0.124622
φ_e (rad)	0.123220	0.160444	0.093847

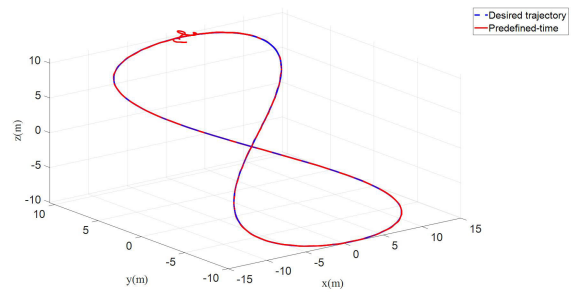

FIGURE 7. 3D trajectory tracking.

the proposed method is able to converge within 5 s in all three directions. Both the proposed method and the method in Reference 2 converge within 5 s, but the proposed method has a shorter convergence time and a smaller stabilization error. Therefore, the proposed H_∞ predefined-time control method can converge quickly within a predefined time, i.e., within 5 s, and does not require complex calculations to derive the convergence time as the fixed-time H_∞ method does. On the other hand, the proposed method has a faster convergence time and better tracking performance than the method proposed in Reference 2.

Fig. 6 shows a comparison of the three LOS errors $\rho_e, \theta_e, \varphi_e$ obtained by the proposed predefined-time H_∞ control method, the fixed-time H_∞ control method proposed in Reference 1, and the predefined-time control method proposed in Reference 2. To see the comparison results more clearly, Table 4 depicts the average error under the three control methods. It can be seen from Fig. 6 that the errors

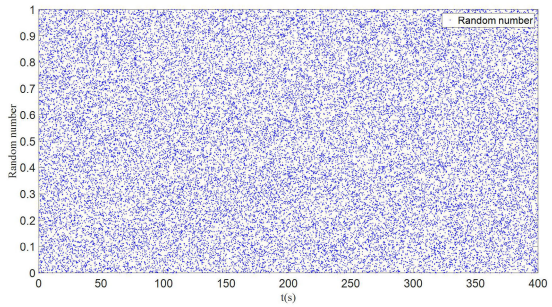

FIGURE 8. Random number.

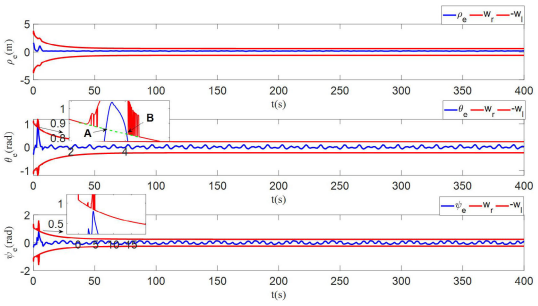

FIGURE 9. Self-adjusting boundary error constraints.

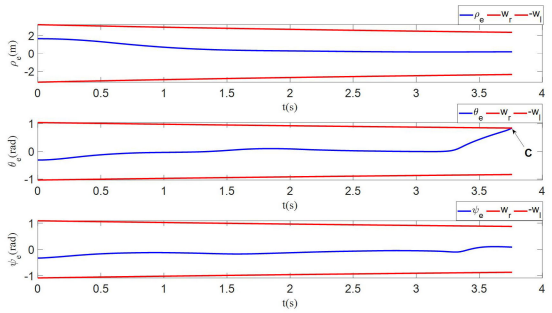

FIGURE 10. Nonadjustable boundary error constraints.

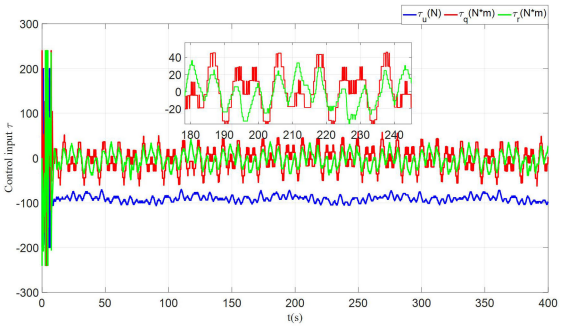

FIGURE 11. Control input.

$\rho_e, \theta_e, \varphi_e$ of the proposed control methods and the method in Reference 2 all converge within 5 s, while the Reference 1 method errors ρ_e, φ_e converge within approximately 15 s. Table 4 clearly shows that the three average errors of the highlighted control methods are 0.236180 m, 0.125622 rad and 0.093847 rad, which are approximately 0.26 m, 0.22 rad and 0.03 rad less than those of the method in Reference 1 and approximately 0.22 m, 0.001 rad and 0.07 rad less than those of the method in Reference 2, respectively. Therefore, the

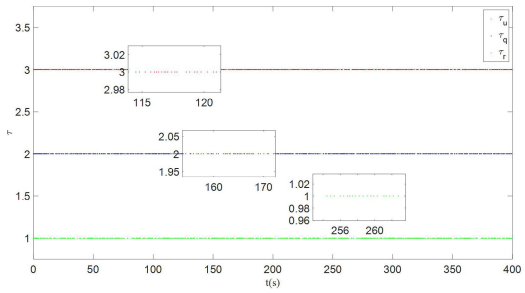

FIGURE 12. Trigger time and trigger interval.

TABLE 5. Event-triggered method.

Force or torque	Sampling number	Number of triggers	Saved resources
$\tau_u(N)$	40001	1169	97.08%
$\tau_q(N \cdot m)$	40001	1201	97.00%
$\tau_r(N \cdot m)$	40001	1527	96.18%

TABLE 6. Comparison of event-triggered methods.

Force or torque	Fixed threshold	Dynamic threshold	Proposed method
$\tau_u(N)$	87.61%	92.39%	97.08%
$\tau_q(N \cdot m)$	81.01%	88.46%	97.00%
$\tau_r(N \cdot m)$	80.51%	91.08%	96.18%

proposed method has faster convergence and smaller tracking errors than the Reference 1 and Reference 2 controllers.

Since AUVs may encounter multiple complications underwater during realistic navigation, the model we used becomes less accurate. Therefore, for a better simulation, unlike the model uncertainty parameter, which is set to a constant value of 0.01 in the literature [6], we set the model uncertainty parameter $\Delta_{d,j}, \Delta_{m,j}(j = 1, 2, 3, 5, 6), \Delta_g$ to a random number between 0 and 1, and it changes randomly at each sampling point. Figs. 7 to 12 show the trajectory tracking effect of the proposed control method with the addition of the random model uncertainty parameter in the presence of the above external disturbance and actuator saturation.

Fig. 7 shows that the proposed controller still enables the AUV to track on the desired trajectory with actuator saturation, a random model uncertainty parameter and an event-triggered method. Fig. 8 represents the random number of model uncertainty parameters between 0 and 1.

Fig. 9 shows that all three errors $\rho_e, \theta_e, \varphi_e$ converge to a steady state in a predefined time. According to the statistical calculations, the average values of the three errors $\rho_e, \theta_e, \varphi_e$ are 0.196804 m, 0.039371 m and 0.067492 m, respectively. At the beginning of the tracking task, the large starting forces and torques of the underactuated system, along with actuator saturation and random model uncertainty, can lead to large errors. When the actuator is saturated and simultaneously has a large position error, the singular value problem is likely to occur. Fig. 10 indicates that when the boundary is immutable, the simulation is not able to continue when the boundary and

the error produce singularity C. Fig. 9 shows that at approximately 3 s, actuator saturation causes the error to suddenly become larger than the original boundary, which is indicated by the green dashed line in the figure. At this time, the green dashed line and the error line appear at the two intersections of point A and point B. Then, the boundary is equal to the error, i.e., the singular value problem appears. The self-adjusting boundary proposed in this paper can eliminate this kind of singular value problem.

It is clear that the control values input into the controller appear in steps under the control of the event-triggered controller and are maintained in the saturation range illustrated in Fig. 11. Fig. 12 represents the trigger time and trigger interval of the event-triggered controller.

According to Table 5, the event-triggered controllers in the three directions saved 97.08%, 97.00% and 96.18% of the communication resources, respectively.

Table 6 provides a comparison of the resources saved by the proposed event-triggered method with the fixed threshold event-triggered method in reference [32] and the dynamic threshold event-triggered method proposed in reference [33]. It is obvious that the proposed event-triggered method can save communication resources compared to both the fixed threshold and dynamic threshold methods.

VI. CONCLUSION

A predefined-time H_∞ trajectory tracking control scheme based on self-adjusting prescribed performance functions and a dynamic relative threshold event-triggered mechanism is proposed for a five-degree-of-freedom underactuated AUV with unknown external disturbances and saturated actuators. The proposed self-adjusting PPC method can constrain tracking errors and eliminate singularity problems when actuators are saturated. Then, a predefined-time H_∞ trajectory tracking controller is proposed to suppress external disturbances and enhance the robustness of the whole system. In addition, a dynamic relative threshold event-triggered mechanism is proposed to effectively reduce the number of transmissions and save communication resources. Finally, the simulations verify the effectiveness and robustness of the proposed control algorithm, which is able to track the desired trajectory within a small error range despite external perturbations and actuator saturation. The proposed control method in this article can only solve the singularity problem caused by actuator saturation, but it cannot solve the singularity problem caused by other problems. Therefore, in the next step, we will study the self-adjusting control method to solve the singularity problems in any situation.

REFERENCES

[1] L. Qiao, B. Yi, D. Wu, and W. Zhang, "Design of three exponentially convergent robust controllers for the trajectory tracking of autonomous underwater vehicles," *Ocean Eng.*, vol. 134, pp. 157–172, Apr. 2017, doi: 10.1016/j.oceaneng.2017.02.006.

[2] K. Shojaei, "Three-dimensional neural network tracking control of a moving target by underactuated autonomous underwater vehicles," *Neural Comput. Appl.*, vol. 31, no. 2, pp. 509–521, Feb. 2019, doi: 10.1007/s00521-017-3085-6.

[3] Y. Li, C. Wei, Q. Wu, P. Chen, Y. Jiang, and Y. Li, "Study of 3 dimension trajectory tracking of underactuated autonomous underwater vehicle," *Ocean Eng.*, vol. 105, pp. 270–274, Sep. 2015, doi: 10.1016/j.oceaneng.2015.06.034.

[4] Z. Yan, M. Wang, and J. Xu, "Robust adaptive sliding mode control of underactuated autonomous underwater vehicles with uncertain dynamics," *Ocean Eng.*, vol. 173, pp. 802–809, Feb. 2019, doi: 10.1016/j.oceaneng.2019.01.008.

[5] O. Elhaki and K. Shojaei, "A robust neural network approximation-based prescribed performance output-feedback controller for autonomous underwater vehicles with actuators saturation," *Eng. Appl. Artif. Intell.*, vol. 88, Feb. 2020, Art. no. 103382, doi: 10.1016/j.engappai.2019.103382.

[6] H. Sun, G. Zong, J. Cui, and K. Shi, "Fixed-time sliding mode output feedback tracking control for autonomous underwater vehicle with prescribed performance constraint," *Ocean Eng.*, vol. 247, Mar. 2022, Art. no. 110673, doi: 10.1016/j.oceaneng.2022.110673.

[7] Z. Yan, M. Zhang, C. Zhang, and J. Zeng, "Decentralized formation trajectory tracking control of multi-AUV system with actuator saturation," *Ocean Eng.*, vol. 255, Jul. 2022, Art. no. 111423, doi: 10.1016/j.oceaneng.2022.111423.

[8] C. Wang, S. Zhu, W. Yu, L. Song, and X. Guan, "Adaptive prescribed performance control of nonlinear asymmetric input saturated systems with application to AUVs," *J. Franklin Inst.*, vol. 358, no. 16, pp. 8330–8355, Oct. 2021, doi: 10.1016/j.jfranklin.2021.08.026.

[9] B. Huang, B. Zhou, S. Zhang, and C. Zhu, "Adaptive prescribed performance tracking control for underactuated autonomous underwater vehicles with input quantization," *Ocean Eng.*, vol. 221, Feb. 2021, Art. no. 108549, doi: 10.1016/j.oceaneng.2020.108549.

[10] M. Zhang, H. Zang, and L. Bai, "A new predefined-time sliding mode control scheme for synchronizing chaotic systems," *Chaos, Solitons Fractals*, vol. 164, Nov. 2022, Art. no. 112745, doi: 10.1016/j.chaos.2022.112745.

[11] S. Xie and Q. Chen, "Adaptive nonsingular predefined-time control for attitude stabilization of rigid spacecrafts," *IEEE Trans. Circuits Syst. II, Exp. Briefs*, vol. 69, no. 1, pp. 189–193, Jan. 2022, doi: 10.1109/TCSII.2021.3078708.

[12] Z. Huang, J. Li, and B. Huang, "Adaptive formation control for autonomous surface vessels with prescribed-time convergence," *Int. J. Adv. Robotic Syst.*, vol. 19, no. 4, Jul. 2022, Art. no. 172988062211057, doi: 10.1177/17298806221105722.

[13] L. Zhang, X. Ju, and N. Cui, "Ascent control of heavy-lift launch vehicle with guaranteed predefined performance," *Aerosp. Sci. Technol.*, vol. 110, Mar. 2021, Art. no. 106511, doi: 10.1016/j.ast.2021.106511.

[14] H. Liu, X. Tian, G. Wang, and T. Zhang, "Finite-time H_∞ control for high-precision tracking in robotic manipulators using backstepping control," *IEEE Trans. Ind. Electron.*, vol. 63, no. 9, pp. 5501–5513, Sep. 2016, doi: 10.1109/TIE.2016.2583998.

[15] Z. Wang, X. Tian, Q. Mai, and H. Liu, "Fixed-time composite robust H_∞ tracking control of marine surface vessels based on the barrier Lyapunov function and an event-triggered strategy," *Ocean Eng.*, vol. 261, Oct. 2022, Art. no. 112113, doi: 10.1016/j.oceaneng.2022.112113.

[16] T. Ma, B. Wang, Z. Zhang, and B. Ai, "A Takagi–Sugeno fuzzy-model-based finite-time H-infinity control for a hydraulic turbine governing system with time delay," *Int. J. Electr. Power Energy Syst.*, vol. 132, Nov. 2021, Art. no. 107152, doi: 10.1016/j.ijepes.2021.107152.

[17] W. Zhang, Y. Teng, S. Wei, H. Xiong, and H. Ren, "The robust H-infinity control of UUV with Riccati equation solution interpolation," *Ocean Eng.*, vol. 156, pp. 252–262, May 2018, doi: 10.1016/j.oceaneng.2018.02.004.

[18] Y. Zhang, M. Zhao, D. Sun, X. Liu, S. Huang, and D. Chen, "Robust H-infinity control for connected vehicles in lattice hydrodynamic model at highway tunnel," *Phys. A, Stat. Mech. Appl.*, vol. 603, Oct. 2022, Art. no. 127710, doi: 10.1016/j.physa.2022.127710.

[19] Q. Mao, L. Dou, Q. Zong, and Z. Ding, "Attitude controller design for reusable launch vehicles during reentry phase via compound adaptive fuzzy H-infinity control," *Aerosp. Sci. Technol.*, vol. 72, pp. 36–48, Jan. 2018, doi: 10.1016/j.ast.2017.10.012.

[20] X. Liu, M. Zhang, and S. Wang, "Adaptive region tracking control with prescribed transient performance for autonomous underwater vehicle with thruster fault," *Ocean Eng.*, vol. 196, Jan. 2020, Art. no. 106804, doi: 10.1016/j.oceaneng.2019.106804.

[21] Z. Guo, D. Henry, J. Guo, Z. Wang, J. Cieslak, and J. Chang, "Control for systems with prescribed performance guarantees: An alternative interval theory-based approach," *Automatica*, vol. 146, Dec. 2022, Art. no. 110642, doi: 10.1016/j.automatica.2022.110642.

[22] J. Xu, Y. Cui, W. Xing, F. Huang, X. Du, Z. Yan, and D. Wu, "Distributed active disturbance rejection formation containment control for multiple autonomous underwater vehicles with prescribed performance," *Ocean Eng.*, vol. 259, Sep. 2022, Art. no. 112057, doi: 10.1016/j.oceaneng.2022.112057.

[23] W. Liu, S. Fei, Q. Ma, H. Zhao, and S. Xu, "Prescribed performance dynamic surface control for nonlinear systems subject to partial and full state constraints," *Appl. Math. Comput.*, vol. 431, Oct. 2022, Art. no. 127318, doi: 10.1016/j.amc.2022.127318.

[24] M.-Y. Li, W.-B. Xie, Y.-L. Wang, and X. Hu, "Prescribed performance trajectory tracking fault-tolerant control for dynamic positioning vessels under velocity constraints," *Appl. Math. Comput.*, vol. 431, Oct. 2022, Art. no. 127348, doi: 10.1016/j.amc.2022.127348.

[25] X. Bu, Q. Qi, and B. Jiang, "A simplified finite-time fuzzy neural controller with prescribed performance applied to waverider aircraft," *IEEE Trans. Fuzzy Syst.*, vol. 30, no. 7, pp. 2529–2537, Jul. 2022, doi: 10.1109/TFUZZ.2021.3089031.

[26] X. Bu, B. Jiang, and Y. Feng, "Hypersonic tracking control under actuator saturations via readjusting prescribed performance functions," *ISA Trans.*, vol. 134, pp. 74–85, Mar. 2023, doi: 10.1016/j.isatra.2022.08.016.

[27] P. Tabuada, "Event-triggered real-time scheduling of stabilizing control tasks," *IEEE Trans. Autom. Control*, vol. 52, no. 9, pp. 1680–1685, Sep. 2007, doi: 10.1109/TAC.2007.904277.

[28] H. Li, J. Pan, X. Zhang, and J. Yu, "Integral-based event-triggered fault estimation and impulsive fault-tolerant control for networked control systems applied to underwater vehicles," *Neurocomputing*, vol. 442, pp. 36–47, Jun. 2021, doi: 10.1016/j.neucom.2021.02.035.

[29] Y. Deng, T. Liu, and D. Zhao, "Event-triggered output-feedback adaptive tracking control of autonomous underwater vehicles using reinforcement learning," *Appl. Ocean Res.*, vol. 113, Aug. 2021, Art. no. 102676, doi: 10.1016/j.apor.2021.102676.

[30] Y. Bian, J. Zhang, M. Hu, C. Du, Q. Cui, and R. Ding, "Self-triggered distributed model predictive control for cooperative diving of multi-AUV system," *Ocean Eng.*, vol. 267, Jan. 2023, Art. no. 113262, doi: 10.1016/j.oceaneng.2022.113262.

[31] Z. Yan, C. Zhang, M. Zhang, J. Yan, and W. Tian, "Distributed event-triggered formation control for multi-AUV system via asynchronous periodic sampling control approach," *Ocean Eng.*, vol. 256, Jul. 2022, Art. no. 111561, doi: 10.1016/j.oceaneng.2022.111561.

[32] H. Liu, Y. Li, X. Tian, and Q. Mai, "Event-triggered predefined-time H_∞ formation control for multiple underactuated surface vessels with error constraints and input quantization," *Ocean Eng.*, vol. 277, Jun. 2023, Art. no. 114294, doi: 10.1016/j.oceaneng.2023.114294.

[33] R. Hao, H. Wang, and W. Zheng, "Dynamic event-triggered adaptive command filtered control for nonlinear multi-agent systems with input saturation and disturbances," *ISA Trans.*, vol. 130, pp. 104–120, Nov. 2022, doi: 10.1016/j.isatra.2022.03.011.

[34] J. Guerrero, J. Torres, V. Creuze, and A. Chemori, "Adaptive disturbance observer for trajectory tracking control of underwater vehicles," *Ocean Eng.*, vol. 200, Mar. 2020, Art. no. 107080, doi: 10.1016/j.oceaneng.2020.107080.

[35] H. Chen, G. Tang, S. Wang, W. Guo, and H. Huang, "Adaptive fixed-time backstepping control for three-dimensional trajectory tracking of underactuated autonomous underwater vehicles," *Ocean Eng.*, vol. 275, May 2023, Art. no. 114109, doi: 10.1016/j.oceaneng.2023.114109.

[36] O. Elhaki and K. Shojaei, "Neural network-based target tracking control of underactuated autonomous underwater vehicles with a prescribed performance," *Ocean Eng.*, vol. 167, pp. 239–256, Nov. 2018, doi: 10.1016/j.oceaneng.2018.08.007.

[37] O. Elhaki, K. Shojaei, and P. Mehrmohammadi, "Reinforcement learning-based saturated adaptive robust neural-network control of underactuated autonomous underwater vehicles," *Expert Syst. Appl.*, vol. 197, Jul. 2022, Art. no. 116714, doi: 10.1016/j.eswa.2022.116714.

[38] Z. Zheng, L. Ruan, and M. Zhu, "Output-constrained tracking control of an underactuated autonomous underwater vehicle with uncertainties," *Ocean Eng.*, vol. 175, pp. 241–250, Mar. 2019, doi: 10.1016/j.oceaneng.2019.02.023.

[39] K. Shojaei and M. Dolatshahi, "Line-of-sight target tracking control of underactuated autonomous underwater vehicles," *Ocean Eng.*, vol. 133, pp. 244–252, Mar. 2017, doi: 10.1016/j.oceaneng.2017.02.007.

[40] K. D. Do, *Control of Ships and Underwater Vehicles Design for Underactuated and Nonlinear Marine Systems*, 1st ed. Cham, Switzerland: Springer, 2009.

[41] K. Shojaei and A. Chatraei, "Robust platoon control of underactuated autonomous underwater vehicles subjected to nonlinearities, uncertainties and range and angle constraints," *Appl. Ocean Res.*, vol. 110, May 2021, Art. no. 102594, doi: 10.1016/j.apor.2021.102594.

[42] G. Che, "Single critic network based fault-tolerant tracking control for underactuated AUV with actuator fault," *Ocean Eng.*, vol. 254, Jun. 2022, Art. no. 111380, doi: 10.1016/j.oceaneng.2022.111380.

[43] Y. Zhang, G. Xia, W. Zhang, K. Zhang, and H. Yang, "Decentralized formation cooperative control for homing of a swarm of underactuated AUVs via singular perturbation," *Ocean Eng.*, vol. 257, Aug. 2022, Art. no. 111577, doi: 10.1016/j.oceaneng.2022.111577.

[44] G. Xia, Y. Zhang, W. Zhang, K. Zhang, and H. Yang, "Robust adaptive super-twisting sliding mode formation controller for homing of multi-underactuated AUV recovery system with uncertainties," *ISA Trans.*, vol. 130, pp. 136–151, Nov. 2022, doi: 10.1016/j.isatra.2022.04.010.

[45] J. Zhang, X. Xiang, L. Lapierre, Q. Zhang, and W. Li, "Approach-angle-based three-dimensional indirect adaptive fuzzy path following of under-actuated AUV with input saturation," *Appl. Ocean Res.*, vol. 107, Feb. 2021, Art. no. 102486, doi: 10.1016/j.apor.2020.102486.

[46] Z. Zuo, M. Defoort, B. Tian, and Z. Ding, "Distributed consensus observer for multiagent systems with high-order integrator dynamics," *IEEE Trans. Autom. Control*, vol. 65, no. 4, pp. 1771–1778, Apr. 2020, doi: 10.1109/TAC.2019.2936555.

[47] Z. Ma and H. Ma, "Adaptive fuzzy backstepping dynamic surface control of strict-feedback fractional-order uncertain nonlinear systems," *IEEE Trans. Fuzzy Syst.*, vol. 28, no. 1, pp. 122–133, Jan. 2020, doi: 10.1109/TFUZZ.2019.2900602.

JIAOYANG ZHUO received the B.E. degree from Guangdong Ocean University, Zhanjiang, China, in 2021, where she is currently pursuing the master's degree with the School of Mechanical Engineering. Her research interests include nonlinear system control, trajectory tracking control of underactuated underwater vehicles, cooperative control, and robust control.

HAITAO LIU (Member, IEEE) received the Ph.D. degree from the School of Mechanical and Automotive Engineering, South China University of Technology, Guangzhou, China, in 2012. He is currently a Professor with the School of Mechanical Engineering, Guangdong Ocean University, Zhanjiang, China. His research interests include the theory and applications of nonlinear control and robotics.

XUEHONG TIAN received the M.E. degree in mechanical engineering from Guangdong Ocean University, Zhanjiang, China, in 2018. She is currently an Associate Professor with the School of Mechanical and Power Engineering, Guangdong Ocean University. Her research interests include robot control, multiagent systems, and nonlinear system design.

QINGQUN MAI received the Ph.D. degree from the School of Mechanical and Automotive Engineering, South China University of Technology, Guangzhou, China, in 2017. She is currently a Lecturer with the School of Mechanical Engineering, Guangdong Ocean University, Zhanjiang, China. Her current research interests include precision manufacturing, intelligent optimization, and marine robotics.